Studies by thermally stimulated current (TSC) of hydroxy- and fluoro-carbonated apatites containing sodium ions

2000 J. Phys.: Condens. Matter 12 8331

(http://iopscience.iop.org/0953-8984/12/38/309)

J. Phys.: Condens. Matter **12** (2000) 8331–8343. Printed in the UK PII: S0953-8984(00)06291-3

Studies by thermally stimulated current (TSC) of hydroxy- and fluoro-carbonated apatites containing sodium ions

H El Feki†, A Ben Salah†, A Daoud†, A Lamure‡ and C Lacabanne‡

† Laboratoire de Chimie du Solide, Faculté des Sciences de Sfax, Tunisia
‡ Laboratoire de Physique des Polymères, Université Paul Sabatier, Toulouse, France

Received 22 July 1999, in final form 26 June 2000

Abstract. Carbonated hydroxyapatites ($HAPCO_3Na$) and fluoroapatites ($FAPCO_3Na$) containing sodium ions have been precipitated by the hydrothermal method.

The effect of carbonate and sodium substituted for phosphate and calcium respectively on the dipolar mobility of the OH^- and F^- ions located inside the apatitic channels of those samples has been studied by thermally stimulated current (TSC). In both apatites two relaxation modes, around -100 and $+50\,^\circ C$, have been observed.

In the $HAPCO_3Na$ sample, the relaxation mode fine structure reveals the existence of two cooperative phenomena with compensation temperatures in the vicinity of the hydroxyapatite monoclinic–hexagonal transition. After preheating of samples at $400\,^\circ C$, the presence of cooperative movements is confirmed by the observation of a compensation phenomenon with a compensation temperature equal to $214\,^\circ C$. An x-ray diffraction study is in agreement with this attribution.

As for the $FAPCO_3Na$ sample, the fine structure of the lower temperature relaxation mode only reveals a compensation phenomenon at $5\,^\circ C$ attributed to water molecule reorientations inside apatitic channels.

1. Introduction

Calcium phosphates, having apatitic structure, constitute the major inorganic component of calcified tissues (bone, tooth, dental enamel) [1–6] and of mineral phosphates. The structure of these apatites can easily accommodate a great variety of substitutions either in the apatitic skeleton or in the channel [7–11]. In particular, hydroxyl ions in hydroxyapatites (HAP) and fluoride ions in fluorapatites (FAP) constitute linear chains inside the apatitic channels [12]. The presence of channels confers to these materials an interesting unidimensional character [13, 14]. According to De Mayer *et al* [15, 16] phosphate ions can be substituted by carbonate ions in at least six mechanisms and in all cases vacancies are created in apatitic structures. Moreover, substitution of some calcium ions by sodium ones creates supplementary vacancies (in calcium sites).

In the 1960s, Bucchi and Fieschi [17, 18], showed that the thermally stimulated current (TSC) can be used to characterize point defects in simple crystals [19]. Later, this dielectric spectrometry was extended to study various materials [19–24]. In particular, Hitmi *et al* [25] have shown that dielectric relaxations in stoichiometric apatites are given by dipolar reorientations inside apatitic channels. Moreover, compensation time and temperature parameters deduced from the analysis of the relaxation fine structure have been correlated with the degree of disorder inside the apatitic structure [26]. Therefore, TSC spectrometry

0953-8984/00/388331+13$30.00

has been chosen to analyse the dipolar movements of sodium-carbonated hydroxy- and fluor-apatites. The aim of this work is to characterize the effect of sodium ions on the hydroxyl or fluoro mobility.

2. Materials and methods

2.1. Preparation of samples

Carbonated apatites containing sodium have been precipitated according to the double decomposition method first described by Legeros [27, 28] and later slightly modified [29]. Briefly, a solution of calcium nitrate (0.03 M) is added drop by drop to a solution heated at 80 °C, containing disodic phosphate (0.008 M) and disodic carbonate concentrated to obtain a $[CO_3^{2-}]/[PO_4^{3-}]$ molar ratio included between 0.5 and 50 l^{-1}. In the case of fluorapatite, ammonium fluoride (0.04 M) was added to the solution.

In the article, carbonated hydroxy- and fluor-apatites containing sodium ions will be labeled HCO_3NaAp and FCO_3NaAp respectively.

2.2. Physico-chemical characterizations

The nature and purity of the samples have been tested by x-ray diffraction (XRD) and infrared absorption spectrometry (IR). IR spectra of the samples dispersed in a potassium bromide tablet were recorded using a Shimadzu IR 470 single beam spectrometer and powder x-ray diffraction analysis was carried out using a Seifert XRD 3000 TT diffractometer controlled by an IBM PC microcomputer and equipped with a diffracted-beam monochromator. To determine the apatitic structures, various chemical analyses have been carried out: the mass calcium content has been determined by complexometric titration with ethylene diamine tetra-acetic acid [30] and 0.9% as estimated standard error. The phosphate content has been determined by colorimetry after complexation with vanadomolybdate [31], with a precision around 0.6%. The sodium content has been measured by atomic absorption with 2% error. As for the carbonate content, it has been deduced from gravimetry, as previously described [32] with an estimated error of 3% and the fluoride one by ionometry with a precision of about 2%. The hydroxyl content has been adjusted by assuming cell electroneutrality. Moreover, the apatite density has been determined by the flotation method [33]. Finally, the unit-cell dimensions of all samples have been calculated by analysis of the x-ray diffraction patterns.

In order to determine the symmetry of the high temperature phase, a powder diffractogram of the sodium carbonated hydroxy-apatite previously heated at 400 °C has been recorded at 230 ± 10 °C, with a Seifert diffractometer equipped with a high temperature cell and the following experimental parameters: 40 s count time, 0.01° angular step and 5°–55° angular range. The diffraction peak position has been determined by a fitting procedure using a pseudo-Voigt function (program: XDAL) [34]. An automatic indexation method has been applied to all different reflections, using the two specific programs DICVOL91 [35, 36] and NBS*AIDS 83 [37].

2.3. TSC experiments

Apatites have been studied with a TSC/RMA spectrometer. The powders were compressed into discs 8 mm in diameter and from 0.5 to 0.8 mm in thickness under a pressure of the order of 10^8 N m^{-2} in vacuum. The disc-shaped specimen was put between the plates of a parallel plate condenser and was polarized by application of a static electric field $E_p = 5 \times 10^5$ V m^{-1}. All complex TSC spectra have been obtained by applying an identical constant electric field

Table 1. Chemical formulae of apatites.

Apatite	Formulae
HCO_3NaAp	$Ca_{8.4}Na_{0.8}(PO_4^{3-})_{3.6}(CO_3^{2-})_{2.4}(OH^-)_2$
FCO_3NaAp	$Ca_{7.91}Na_{1.57}(PO_4^{3-})_{3.39}(CO_3^{2-})_{2.61}(F^-)_2$

Table 2. Crystallographic parameters (±0.003 Å) determined at room temperature of apatites previously heated at T_t.

Apatite	$T_t = 200\,^\circ$C	$T_t = 400\,^\circ$C
HCO_3NaAp	$a = 9.362$ $c = 6.910$	$a = 9.325$ $c = 6.921$
FCO_3NaAp	$a = 9.254$ $c = 6.911$	$a = 9.247$ $c = 6.919$

E_p, at a given polarization temperature T_p chosen to magnify dipolar relaxations. Then, the sample was cooled down under field until the liquid nitrogen temperature T_d. After removal of the field, the depolarization current was recorded with a linear increase of temperature of 7 K min^{-1}. In all apatites, the dielectric relaxations are complex, implying the existence of a distribution of relaxation times.

To determine the origin of these movements, spectra have been experimentally decomposed into a series of elementary peaks by using the fractional polarization method [38]. The electric field is applied on a narrow polarization window $\Delta T = T_p - T_d = 10$ K. With this procedure, only entities with relaxation time included between $\tau(T_p)$ and $\tau(T_d)$ can relax. So, the depolarization current is recorded by using the same protocol as for complex spectra. Finally, in order to resolve the whole TSC spectrum into a series of elementary processes, the polarization window is shifted, by a constant step of 10 K, along the temperature axis.

3. Results

Crystallographic and physico-chemical studies show that all precipitated products are constituted by pure apatites and are containing sodium and carbonate ions.

The infrared absorption spectra (figure 1) of both compounds are typical of B-type carbonate containing apatites [39] with the CO_3^{2-} bending vibration observed at about 871 cm^{-1} and the CO_3^{2-} stretching vibrations at about 1420 and 1460 cm^{-1}. The absorptions in the ranges 970–1100 and 565–615 cm^{-1} are attributed to the PO_4^{3-} vibrations. But in the case of HCO_3NaAp spectrum there exists, indeed, the stretching and libration modes of OH^- ions at around 3560 and 633 cm^{-1} and the shoulder at 740 cm^{-1} attributed to the ν_L mode of OH^- close neighbours to the Na^+ ion [40]. Moreover, chemical analyses complemented by XRD study have allowed us to determine the chemical formulae and the crystallographic parameters of these apatites. These results are reported in tables 1 and 2 respectively.

3.1. HCO$_3$NaAp dielectric relaxations

Before the TSC study, the HCO_3NaAp samples were heated to 200 °C for 1 hour, to eliminate adsorbed water without affecting the crystallographic parameters [11]. The electric field was applied at 50 °C, and the depolarization current recorded between −170 and 160 °C. The corresponding complex spectrum, represented in figure 2, shows the existence of two peaks: the first around −90 °C and the second centred at 40 °C. By using the fractional polarization procedure, between −160 and 100 °C, the fine structure of dielectric relaxation has been obtained. As

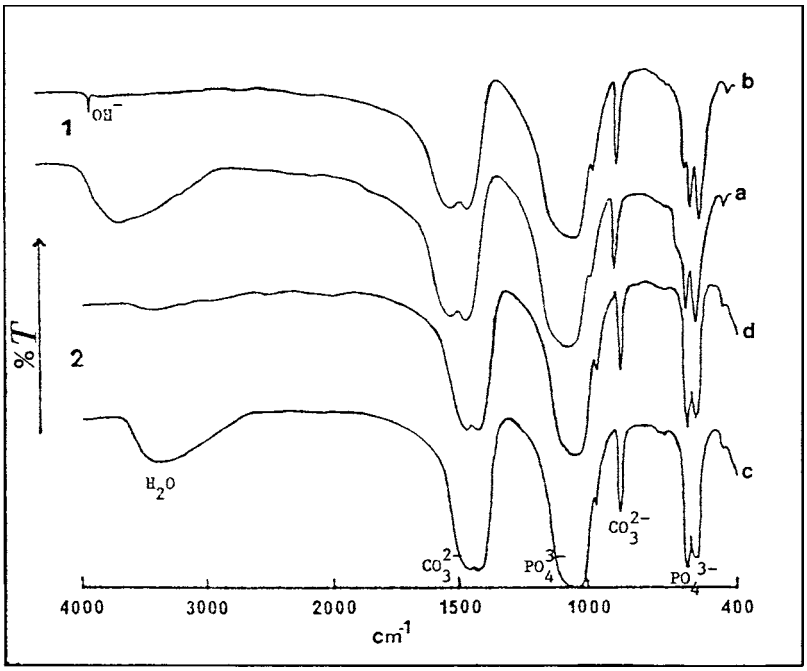

Figure 1. IR spectra of the sodium carbonated hydroxy- $HCaCO_3Na$ (1) and fluor-apatites FCO_3Na (2) preheated at $T_t = 200$ (a), (c) and 400 °C (b), (d).

shown in figure 3(a) and (b), the elementary spectrum envelope reproduces the same variation as the complex spectrum. The variation, with temperature, of each relaxation time corresponding to one elementary peak has been deduced from the relation $\tau(T) = P(T)/J(T)$ where $P(T)$ is the remaining polarization at temperature T and J the corresponding current density.

According to the Arrhenius diagram presented in figure 4, the temperature variation of all relaxation time can be considered as correctly described by an Arrhenius equation: $\tau(T) = \tau_0 \exp(\Delta H/kT)$ where ΔH is the activation energy, τ_0 the pre-exponential factor and k the Boltzmann constant. The Arrhenius parameters, deduced from the analysis of each elementary peak, are reported in table 3. Since the relaxation time corresponds to the frequency reciprocal of a jump between two activated states, the previous empirical equation can be considered analogous to the relation deduced from the Eyring theory of activated states [41]: $\tau(T) = (h/kT) \exp -(\Delta S/k) \exp(\Delta H/kT)$ where ΔH and ΔS are the activation enthalpy and entropy respectively and h is the Planck constant.

Moreover, as shown in figure 4, extrapolation of some relaxation times shows that they converge towards particular points. The corresponding relaxation times included in a spindle (dotted lines in figure 4) also obey a compensation law:

$$\tau(T) = \tau_c \exp \frac{\Delta H}{k} \left(\frac{1}{T} - \frac{1}{T_c} \right)$$

where T_c and τ_c are the compensation temperature and time respectively. This relation shows that when the temperature T is equal to the compensation temperature T_c, all relaxations take the same time τ_c, indicating a cooperativity of molecular motions [22, 23, 42]. In the HCO_3Na apatite, two compensation phenomena, labelled C_1 ($T_{c_1} = 170$ °C, $\tau_c = 10^{-7}$ s) and C_2 ($T_{c_2} = 190$ °C, $\tau_c = 10^{-6}$ s) on the Arrhenius diagram, can be observed (figure 4). The

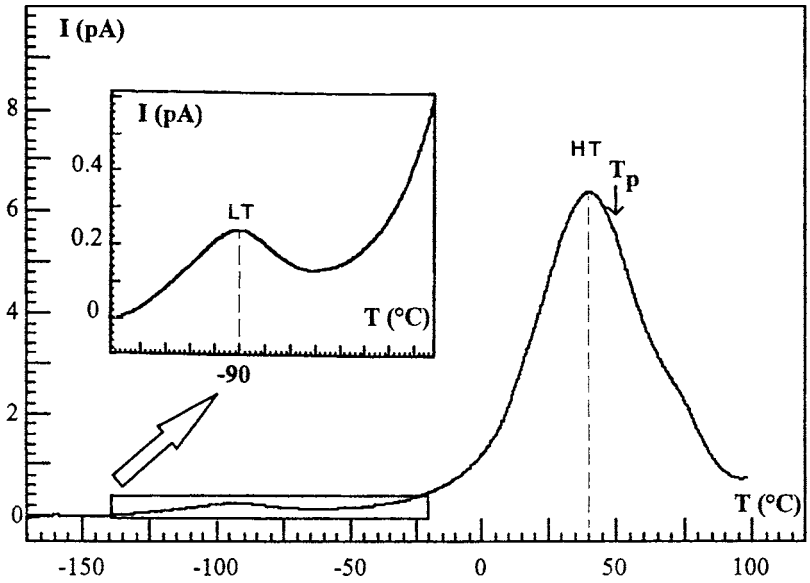

Figure 2. Complex TSC spectrum of the HCO_3NaAp sample preheated at $T_t = 200\,^{\circ}C$.

Table 3. Arrhenius parameters of the $HCaCO_3NaAp$ sample previously heated at $T_t = 200\,^{\circ}C$.

T_{max} (°C)	ΔH (eV)	τ_0 (s)	Compensation point
−138.9	0.37	6.9×10^{-13}	
−128.5	0.43	4.0×10^{-14}	
−119.5	0.48	4.4×10^{-15}	
−114.7	0.42	2.5×10^{-12}	C_1[a]
−104.1	0.47	3.3×10^{-13}	C_1
−95.5	0.52	1.0×10^{-13}	C_1
−84.5	0.58	1.8×10^{-14}	C_1
−75.9	0.62	6.8×10^{-15}	C_1
−65.5	0.66	3.8×10^{-15}	C_1
−55.1	0.73	5.2×10^{-16}	C_1
−44.1	0.67	9.3×10^{-14}	
−36.5	0.78	1.2×10^{-15}	
−22.1	0.85	3.5×10^{-16}	
−14.3	0.79	2.2×10^{-14}	C_2[b]
−4.3	0.86	4.8×10^{-15}	C_2
+5.9	0.92	1.4×10^{-15}	C_2
17.5	1.03	8.7×10^{-17}	C_2
31.1	1.17	1.7×10^{-18}	C_2
35.9	0.97	1.1×10^{-14}	
47.1	1.03	3.6×10^{-15}	

[a] C_1: $T_{c_1} = 170\,^{\circ}C$, $\tau_c = 10^{-7}$ s.
[b] C_2: $T_{c_2} = 190\,^{\circ}C$, $\tau_c = 10^{-6}$ s.

first compensation phenomenon is constituted by the elementary peaks 5 to 11 and the second one by elementary processes isolated between −20 and 30 °C. Corresponding compensation parameters, characteristic of the dynamic molecular movements are reported in table 3.

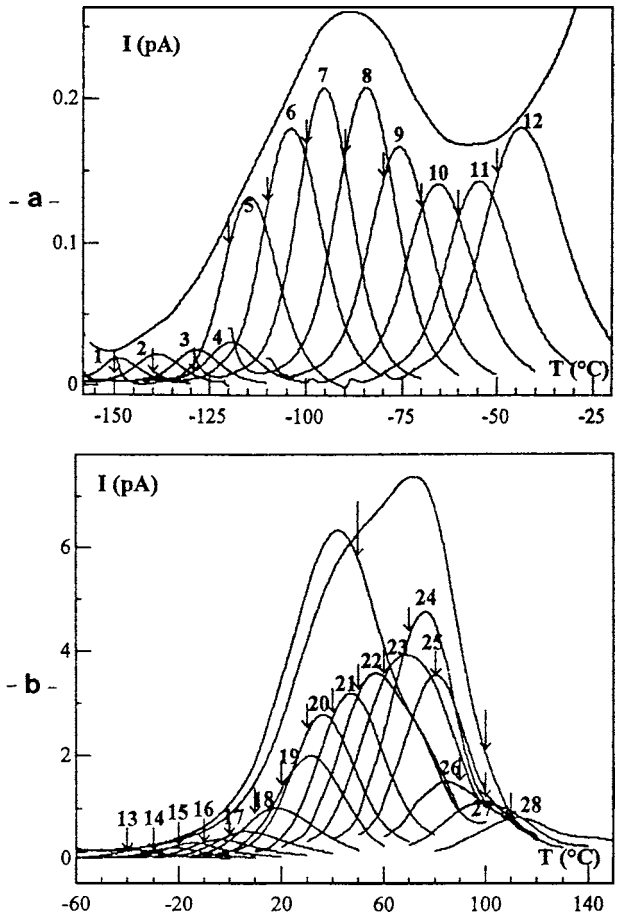

Figure 3. Elementary TSC spectra of the HCO_3NaAp sample preheated at 200 °C: (a) low temperature mode and (b) high temperature mode.

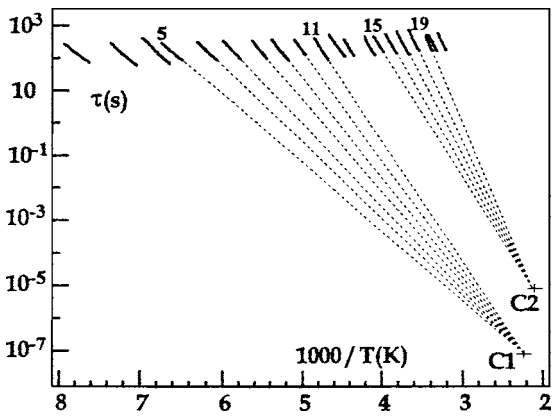

Figure 4. Arrhenius diagram of the relaxation time isolated in the HCO_3NaAp sample preheated at $T_t = 200$ °C.

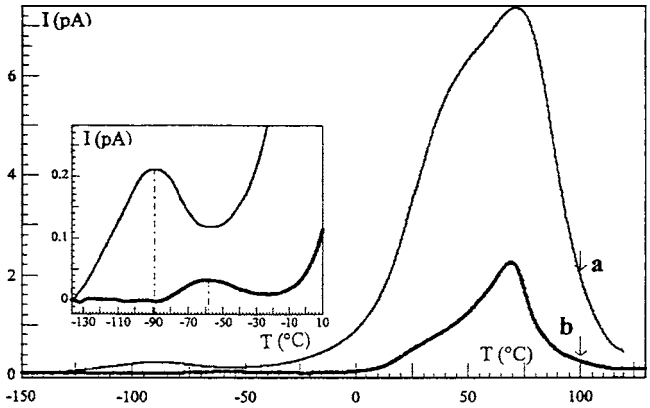

Figure 5. Complex TSC spectra of the HCO_3NaAp sample preheated at (a) $T_t = 200\,^{\circ}$C and (b) $T_t = 400\,^{\circ}$C.

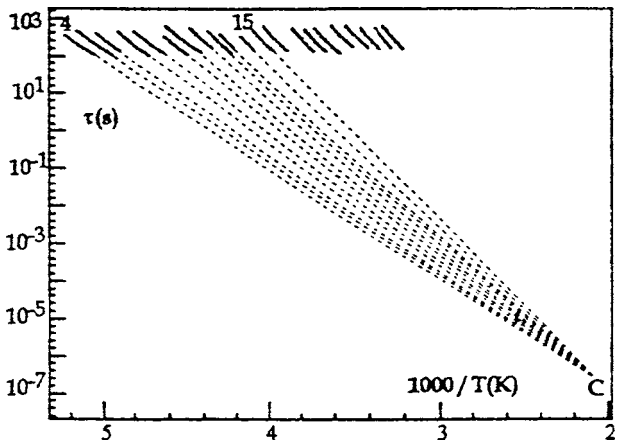

Figure 6. Arrhenius diagram of the relaxation times isolated in the HCO_3NaAp sample preheated at $T_t = 400\,^{\circ}$C.

In order to determine the origin of this second process and discriminate the influence of water, a complementary study has been performed on the same apatite, after a pretreatment of the sample at 400 °C for 24 h, under secondary vacuum (10^{-6} Torr). After pretreatment, the sample was then studied with the same polarization protocol (field intensity and temperature) as previously. The corresponding spectrum represented in figure 5 superposed with the non-preheated spectrum confirms the existence of two relaxation modes. However the depolarization intensity is significantly decreased and the lower temperature mode is shifted towards higher temperature after the 400 °C pretreatment.

Moreover, by using the fractional polarization procedure, the dehydrated sample spectrum has been decomposed in a series of elementary spectrum. Figure 6 represents the temperature variation of the corresponding relaxation times. In that case, only one point of convergence labelled C is observed. The single compensation phenomenon corresponds to the cooperativity of elementary phenomena isolated in the lower temperature mode. The corresponding compensation parameters are: $T_c = 214\,^{\circ}$C and $\tau_c = 10^{-7}$ s.

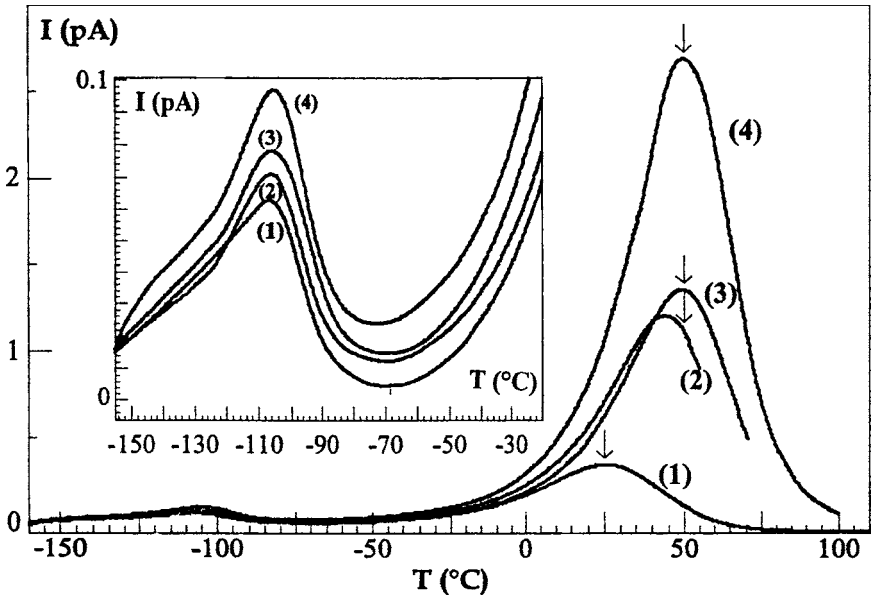

Figure 7. Complex successive TSC spectra of the FCO_3NaAp sample preheated at $T_i = 200\,^{\circ}C$. (1) $T_p = 25\,^{\circ}C$ and (2)–(4) $T_p = 50\,^{\circ}C$.

3.2. FCO_3NaAp dielectric relaxations

After sample heating at 200 °C, several successive scans, at different polarization temperatures, have been performed. As for the previous carbonated hydroxy-apatite, the complex spectrum of the carbonated fluor-apatite presents two main relaxation modes (cf figure 7). A lower temperature, the peak that appears in the vicinity of −110 °C is less intense than the corresponding HCO_3NaAp one. As for the higher temperature mode, its maximum varies in position and intensity with successive runs. These evolutions can be probably associated with a water loss when the sample is heated over 100 °C.

To determine the origin of the lower temperature mode, the fractional polarization procedure has been applied. As shown in figure 8, all relaxation times corresponding to elementary processes isolated between −150 and −50 °C obey an Arrhenius law. Moreover, the first eight relaxation times are described by a compensation phenomenon, labelled C′, with the following parameters: $T_{c'} = 5\,^{\circ}C$ and $\tau_{c'} = 10^{-5}$ s.

4. Discussion

4.1. Origin of the FCO_3NaAp dielectric relaxations

The TSC spectra of the FCO_3NaAp preheated at 200 °C have shown a lower temperature relaxation around −110 °C. Analysis of this mode reveals that it is constituted by cooperative movements with a compensation temperature equal to 5 °C. Complementary analysis of the fine structure of the FCO_3NaAp preheated at 400 °C demonstrates the total disappearance of cooperative movements after the thermal treatment.

Moreover, the study of IR spectra at 200 °C shows the presence of a large band at about 3500 cm^{-1} and attributable to H_2O. This band disappears from the IR spectrum after heating of the sample at 400 °C. Finally, XR diffraction reveals that the cell parameter

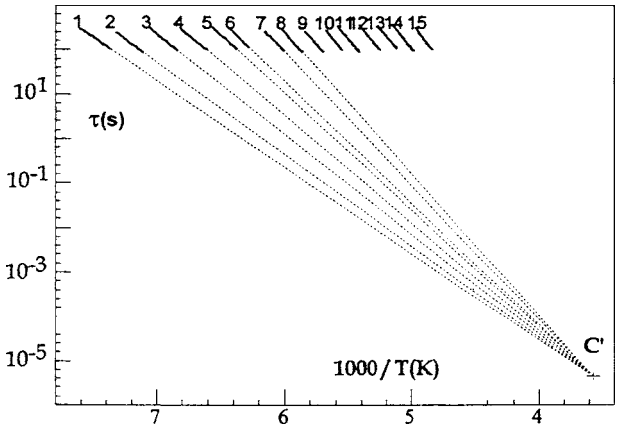

Figure 8. Arrhenius diagram of the relaxation times isolated in the FCO$_3$NaAp sample preheated at $T_t = 200\,^{\circ}$C.

a decreases between 200 and 400 °C (table 2). These results clearly show that water molecules which are present in the substituted apatite correspond to structural water molecules. Water molecules could be located in either the oxygen or calcium vacancies, as reported previously.

So the cooperative dielectric movements observed in the FAPCO$_3$Na apatite preheated at 200 °C have been attributed to OH dipoles relaxations of structural water molecules. This interpretation is in good agreement with previous studies in collagen. As shown by Mezghani *et al*, bound water molecules located inside the collagen triple helix are also characterized by a compensation phenomenon with a compensation temperature in the vicinity of the ice–liquid transition [43].

4.2. Origin of the HCO$_3$NaAp dielectric relaxations

First, taking into account differences between the relaxation temperature maxima and the $T_{c'}$ values, it seems logical to think that movements implied in the two apatitic samples have different origins.

In the case of HCO$_3$Na apatite preheated at 200 °C, a double compensation phenomenon is observed. The existence of two types of relaxation as in enamel [26] could imply the existence of two segregated phases. After preheating the sample at 400 °C, only one compensation phenomenon subsists (cf figure 9). It is well known that one effect of apatitic substitutions is the creation of vacancies in calcium sites, in which water molecules can lodge [8, 11]. Moreover, as in the FCO$_3$Na apatites, IR absorption and XR diffraction studies confirm the existence of water in HCO$_3$Na apatites preheated at 200 °C which disappears after sample heating at 400 °C. These observations lead us to attribute the lower temperature mode to OH dipole relaxations of structural water molecules. However, the comparison between the compensation temperatures corresponding to the water molecules cooperative relaxation in the FCO$_3$Na and the HCO$_3$Na apatites preheated at 200 °C (5 and 170 °C respectively) demonstrates that structural water can present different dynamics. On one hand, in the FCO$_3$Na apatite, the value is practically equal to the ice–water transition: the dielectric relaxation could be associated with free water molecule movement. On the other hand, in the HCO$_3$Na apatite, the value is similar to the monoclinic–hexagonal transition temperature from a non-stoichiometric apatite. In that case, the water molecule could located inside apatitic channels and the dielectric relaxation could

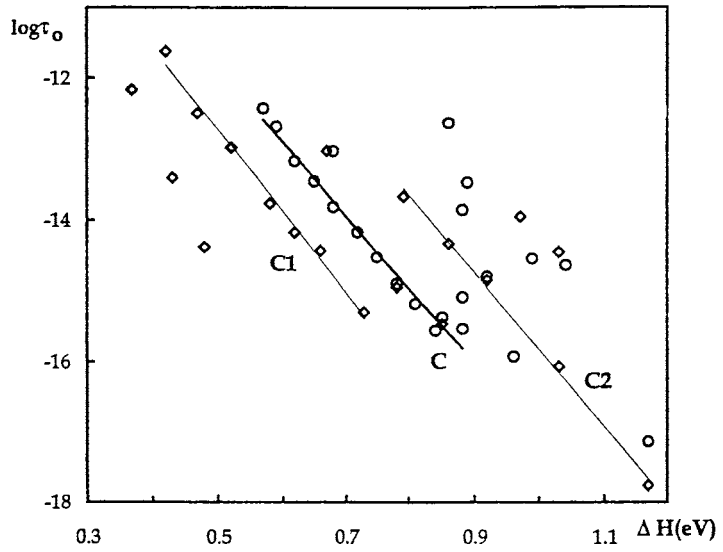

Figure 9. Compensation diagram of the $HCaCO_3NaAp$ sample previously heated at: square, $T_t = 200\,^{\circ}C$ and circle, $T_t = 400\,^{\circ}C$.

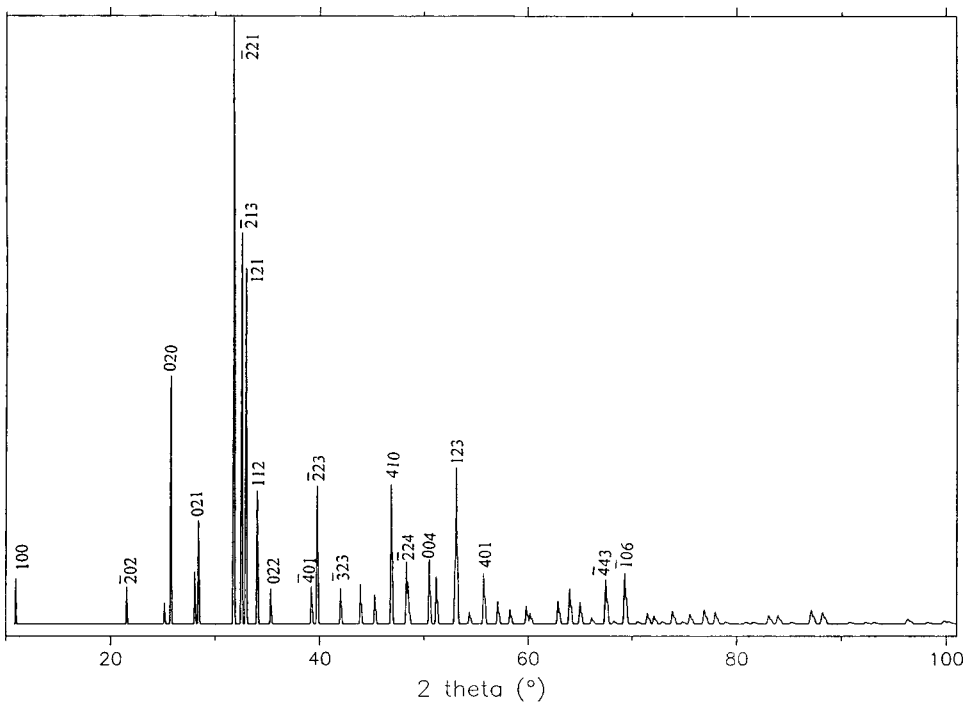

Figure 10. X-ray diffraction pattern at $230\,^{\circ}C$ of the $HCaCO_3NaAp$ sample previously heated at $400\,^{\circ}C$ (spectrum simulated according to experimental angles and intensities).

be due to OH dipole inversion in the neighbourhood of the water molecule, according to the Elliott *et al* representation [14].

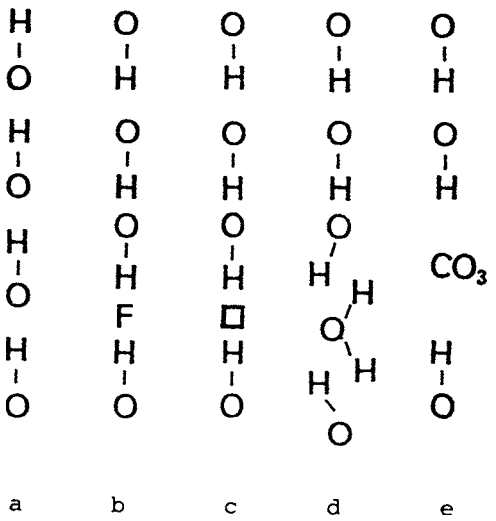

Figure 11. Ion disposition in the channels of apatites according to Elliott *et al* [14]. (a) Arranged column. (b) OH dipole inversion in neighbourhood of F^- ion. (c) OH dipole inversion in neighbourhood of lacuna. (d) OH dipole inversion in neighbourhood of water molecule. (e) OH dipole inversion in neighbourhood of CO_3^{2-} ion.

As for the second relaxation mode, it can be associated with hydroxyl reorientations inside apatitic channels. This interpretation is in good agreement with previous studies of Hitmi *et al*, which have observed a split of the compensation phenomena and a decrease of the compensation temperature between 211 °C, in stoichiometric hydroxyapatite, and 140 °C, in non-stoichiometric hydroxyapatites [25, 44]. The increase of compensation temperature between the HCO_3Na apatites preheated at 200 °C and at 400 °C (190 and 214 °C respectively) is probably due to the decrease of channel diameter (cf cell parameter a, table 2). After preheating at 400 °C, the compensation temperature of the HCO_3Na apatite is practically equal to the hydroxyapatite monoclinic–hexagonal transition temperature. However, differences in compensation times ($\sim 10^{-3}$ s in stoichiometric hydroxyapatite, 10^{-7} s in HCO_3Na apatite) indicate the existence of disorder in the sodic carbonic apatites.

To confirm the hypothesis that the compensation phenomenon observed in different apatites (arseno-stronsic, arseno-calcic, stronsic orthophosphates ...) is associated with a structural monoclinic–hexagonal transition [25, 44–46], Hiroyk [47] demonstrates a similar transition using the DSC technique. X-ray diffraction experiments have been performed to verify that the studied samples could present a monoclinic structure. Results obtained have confirmed that they can be described by a monoclinic symmetry, with the following cell parameters: $a = 9.722(3)$ Å, $b = 6.912(3)$ Å, $c = 9.029(3)$ Å, $\beta = 123.83°$, $P2/m$. Moreover, values of merit figures M_{20} [48] = 61 and F_{30} [49] = 59, are in good agreement with that solution. From a crystallographic point of view, the transition can be explained by a passage from the $P6_3/m$ group (ambient phase) through the higher symmetry $P6_3/mmm$ group toward the higher temperature phase $P2/m$ monoclinic subgroup (cf figure 10). Therefore, at the transition temperature, a structural rearrangement could exist between OH^- ions of a given channel, leading to the orientation of all ions in the same sense without moving the orientation symmetry of these dipoles through the $b/2$ plane. This interpretation could explain the appearance of the monoclinic structure. Therefore, the passage of the monoclinic structure toward the hexagonal one (vacancies are found in the calcium site (II) that surrounded the OH

chain [50, 51] corresponds to a simple disorder–order transition and only the disordered column model) (cf figure 11) [14], in the hexagonal structure, is in agreement with this transition.

5. Conclusion

This study of sodic carbonated hydroxyapatite by TSC spectrometry has shown two types of behaviour according to the thermal treatment. After preheating at 200 °C, the two compensation phenomena observed have been associated with hydroxyl dipole reorientations, and the splitting to the existence of two different environments, as in dental enamel. After preheating to 400 °C, the single compensation phenomenon observed has been attributed to the dielectric manifestation of a structural hexagonal–monoclinic transition. The existence of a structural hexagonal–monoclinic transition has been confirmed by the XR diffraction study at high temperature. In sodic carbonated fluorapatite preheated at 200 °C, XR diffraction patterns have confirmed the absence of hydroxyl dipoles. In that sample, the cooperative relaxation observed by TSC experiments has been attributed to free water movements.

Acknowledgments

The authors thank Dr S Mezghani for her experimental assistance at the Polymer Physics Laboratory (Toulouse), and Professor M Jemal at the Tunis Science Faculty for his helpful discussion.

References

[1] Fourman P and Royer P 1970 Calcium et tissu osseux *Biologie et Pathologie* (Paris: Flammarion) p 23
[2] Wollest R and Burmy G 1971 *Calcif. Tissue Res.* **8** 73
[3] Montel G, Bonel G, Heughebaert J C, Trombe J C and Rey C 1981 *J. Cryst. Growth* **53** 74
[4] Biltz R and Pellegrino E D 1981 *Mineral Electrolyte Metal.* **5** 1
[5] Driessens F C and Verbeeck R M 1990 *Biominerals* (Boca Raton, FL: Chemical Rubber Company)
[6] Elliot J C 1994 Structure and chemistry of the apatite and other calcium orthophosphates *Studies in Organic Chemistry* (Amsterdam: Elsevier) p 18
[7] Wright G and Montel G 1969 *C.R. Acad. Sci. Paris* **268** 2077
[8] Vignoles C, Bonel G and Montel G 1975 *C.R. Acad. Sci. Paris* **280** 361
[9] Grisafe D A and Hummel F A 1970 *J. Solid-State Chem.* **2** 160
[10] Montel G, Bonel G, Trombe J C, Heughebaert J C and Rey C 1978 *1st Congr. Int. sur les Composés Phosphorés (Rabat)* (Paris) vol 43, 321
Montel G, Bonel G, Trombe J C, Heughebaert J C and Rey C 1980 *Pure. Appl. Chem* **52** 973
[11] Vignoles C, Bonel G and Young R A 1987 *Calcif. Tissue Int.* **40** 64
[12] Sudarsanan K and Young R A 1969 *Acta Crystallogr.* B **25** 1534
[13] Kay M I, Young R A and Posner A S 1964 *Nature* **205** 1050
[14] Elliott J C and Mackie P E 1973 *Coll. Int. CNRS* **230** 69
[15] De Mayer E A, Verbeeck R M and Naessens D E 1993 *Inorg. Chem.* **32** 5709
[16] De Mayer E A and Verbeeck R M 1993 *Bull. Soc. Chim. Belg.* **102** 601
[17] Bucci C and Fieschi R 1964 *Phys. Rev. Lett.* **12** 16
[18] Bucci C, Fieschi R and Guidi G 1966 *Phys. Rev.* **148** 816
[19] Chatain D, Gautier P and Lacabane C 1973 *J. Polym. Sci. Phys. Edn.* **11** 1631
[20] Bernes A, Boyer R F, Lacabane C and Ibar J P 1986 *Order in the Amorphous State of Polymers* ed S E Keinath, R L Miller and J K Ricke (New York: Plenum) p 305
[21] Lavergne C and Lacabane C 1993 *IEEE Elec. Insul. Magn.* **9** 5
[22] Lacabane C, Lamure A, Teyssedre G, Bernes A and Mourgues M 1994 *J. Non-Cryst. Solids* **172–174** 884
[23] Teyssedre G, Mezghani M, Bernes A and Lacabane C 1996 *Dielectric Spectroscopy of Polymeric Materials* ed J Runt and J Fitzgerald (ACS)
[24] Prieto Valdes J J, Victorero Rodriguez A and Guevaro Carrio J 1995 *J. Mater. Res.* **10** 9

[25] Hitmi N, Lacabane C and Young R A 1988 *J. Phys. Chem. Solids* **49** 541
[26] Hitmi N, Lamure-Plaino E, Lamure A, Lacabane C and Young R A 1986 *J. Dental Res.* **10** 9
[27] Legeros R Z 1965 *Nature* **206** 403
[28] Legeros R Z 1967 *PhD Thesis* New York
[29] El Feki H 1990 *Thèse de Spécialité* Tunis
[30] Charlot G 1966 *Les Méthodes de la Chimie Analytique* 5th edn (Paris: Masson)
[31] Gee A and Deitz V R 1953 *Anal. Chem.* **25** 1320
[32] El Feki H and Jemal M *Analysis* **17** 460
[33] Marraha M 1989 *Thèse d'Etat* (Toulouse: INP)
[34] 1994 *XDAL 3000* Seifert x-ray diffraction software (Ahrensburg: Seifert)
[35] Louër D and Louër M J 1972 *J. Appl. Crystallogr.* **5** 272
[36] Bultif A and Louër D 1991 *J. Appl. Crystallogr.* **24** 987
[37] Mighell A D, Hubbard C R and Stalik J K J 1981 *NBS*AIDS80: a FORTRAN Program for Crystallographic Data Evaluation* (NBS)
[38] Ibar J P 1993 *Fundamentals of Thermally Stimulated Current and Relaxation Map Analysis* (New Canaan, CT: SLP) p 67
[39] El Feki H, Rey C and Vignoles M 1991 *Calcif. Tissue Int.* **49** 269
[40] Vignoles C, Trombe J C, Bonel G and Montel G 1975 *C. R. Acad. Sci. Paris* C **280** 275
[41] Eyring H 1944 *J. Chem. Phys.* **4** 283
[42] Teyssedre G, Bernes A and Lacabane C 1995 *J. Polym. Sci. Phys. Edn* **33** 879
[43] Mezghani S, Lamure A and Lacabane C 1995 *J. Polym. Sci. Phys. Edn* **33** 2413
[44] Teyssedre G and Lacabane C 1995 *J. Phys. D: Appl. Phys.* **28** 1479
[45] Hitmi N, Lacabane C and Young R A 1986 *J. Phys. Chem. Solids* **47** 533
[46] Hitmi N, Lacabane C, Bobel G, Roux P and Young R A 1986 *J. Phys. Chem. Solids* **47** 507
[47] Hiroyk S, Masatomo Y, Masata K and Masahiro Y 1995 *J. Phys. C: Solid State Phys.* **99** 6752
[48] De Wolff P M 1986 *J. Phys. Cryst.* **1** 108
[49] Smith G S and Snyder R L 1986 *J. Phys. Cryst.* **12** 60
[50] El Feki H, Savariault J M and Ben Salah A 1999 *J. Alloys Compounds* **287** 114
[51] El Feki H Savariault J M, Ben Salah A and Jemal M *Eur. J. Solid State Inorg. Chem.* submitted